Fatigue in the Core of Aluminium Honeycomb Panels: Lifetime Prediction compared to Fatigue Tests

Laurent Wahl, Stefan Maas, Danièle Waldmann: University of Luxembourg, Campus Kirchberg, Luxembourg

Arno Zürbes: FH Bingen, Germany

Patrick Frères: Eurocomposites, Echternach, Luxembourg

Abstract:

In comparison to their weight, honeycomb composite structures have a high bending stiffness, which makes them very suited for every application where little weight is important, like airplanes, railway-cars and vehicles. The sandwich panels consist of two thin and stiff aluminium face sheets , which are bonded to a thick and lightweight aluminium honeycomb core. These structures are subjected to dynamic loading. However, in literature, there are hardly any fatigue properties of the honeycomb core described. The fatigue properties of the core are investigated using the finite element method and experiments.

Depending on the load application, the honeycomb core fails either through core indentation or shear failure. For a fatigue prediction, both failure modes have to be investigated. Additionally the physical behavior of the honeycomb core is depending on the orientation of the core. Hence, fatigue tests were conducted in three directions of the core: the stiffest direction, the most compliant direction and the direction with the highest stresses.

A three-point bending test setup was built to study the fatigue properties of the honeycomb core. Several fatigue tests were carried out with a load ratio of R=0.1 (maximum load 10 times bigger than minimum load) and the fatigue diagrams being illustrated. Additionally, Food-Cart Roller Tests (wheels of a cart rolling in a circle on a floor panel) were done to dynamically test the panels in every angle.

The sandwich structures were modeled with the ANSYS finite element software. The simulations, which were used to determine the stress amplitudes in the specimens, are described in the following pages. In addition, buckling analyses were used to examine core indentation failure.

Based on these simulations, failure predictions can be made. The fatigue life of the examined specimens is successfully approximated in this manuscript, with the lifetime analysis being based on the FKM-guideline (error less than 14% in load amplitude).

Keywords:

Fatigue, lifetime prediction, aluminium sandwich structure, honeycomb core, out-of-plane shear failure, buckling, FEM, ANSYS, Food-Cart Roller test, FKM guideline

1 Introduction

1.1 Description

Honeycomb composite structures are usually used for applications where low weight is important, like airplanes, railway-cars and vehicles, because of the high bending stiffness in comparison to the low weight. The sandwich panels consist of two thin and stiff aluminium face sheets bonded to a thick and lightweight aluminium honeycomb core. (Fig. 1)

The mechanics of honeycomb sandwich structures have been studied by different authors in the past. Gibson and Ashby [1] conducted a study about the in-plane and out-of-plane stiffness of honeycomb cores. Staal *et al.* [2] investigated different failure modes of bended honeycomb panels. Zhang and Ashby [3] analyzed the out-of-plane properties of honeycombs. Theoretical stresses and buckling loads are derived in L-, W- and T-direction.

Honeycomb structures are usually subjected to dynamic loading. In literature, there have been conducted some experimental investigations, but hardly any stimulation-based fatigue predictions have been made though. Sharma *et al.* [4] presented a summary of the latest update concerning fatigue in honeycomb and foam-cored sandwich panels. Burman and Zenkert [5] investigated experimentally the fatigue properties of pre-damaged and undamaged honeycomb beams. Belouettar *et al.* [6] conducted an experimental study about the static and dynamic failure of honeycomb sandwich structures. Fatigue studies leading to debonding failure were conducted by Belingardi *et al.* [7] and by Berkowitz and Johnson [8]. Fatigue failure in the face sheet of sandwich structures was investigated by Bauer [9]. Bianchi *et al.* [10] made fatigue analyses with honeycombs subjected to in-plane shear stresses, loading the core in different directions. They found out that the shear strength is minimal at an angle between 50° and 80°.

During this project, fatigue tests with failures of the core structure were conducted in parallel with finite element calculations. Tests and simulations were done in the stiffest direction, the most compliant direction and the direction with the highest stresses. It was shown that fatigue life predictions can be made by using finite element simulations and the FKM-guideline [11].

The FKM-guideline can be used for aluminium or steel components of any shape (with or without welds) in mechanical engineering and related fields. Fatigue predictions can be made by using nominal stresses (mainly used for rod-shaped components) or by using local stresses (for example of a finite element simulation, as in this work). The fatigue calculation can be used to determine the initiation of cracks for cycle numbers over 10^4. The FKM-guideline is admissible for temperatures between -25° C and 200° C.

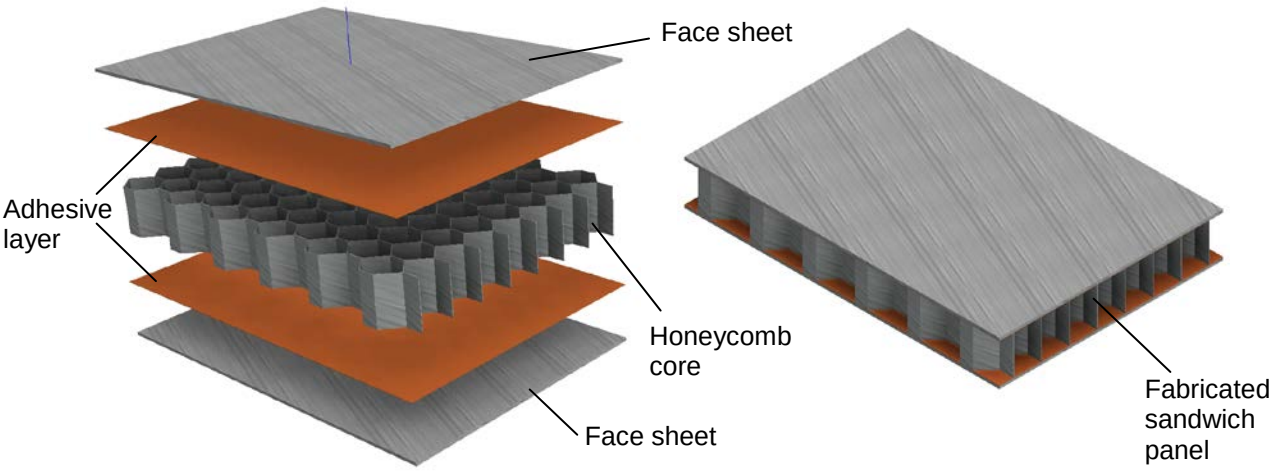

Fig. 1: Sandwich structure with honeycomb core

1.2 Orientation of the Honeycomb Core

Since the behavior of the panels is orthotropic, the panels react differently depending on the direction of the loading. So it is necessary to distinguish between the honeycomb core's three directions of symmetry called L, W and T direction (Fig. 2). The other directions can be specified by the angle α, with α=0° in L-direction and α=90° in W-direction.

The walls of the honeycomb cells have different wall thicknesses. This is due to the manufacturing process, during which the foils are partly glued together. The glued walls with double thickness are in L-direction (Fig. 2).

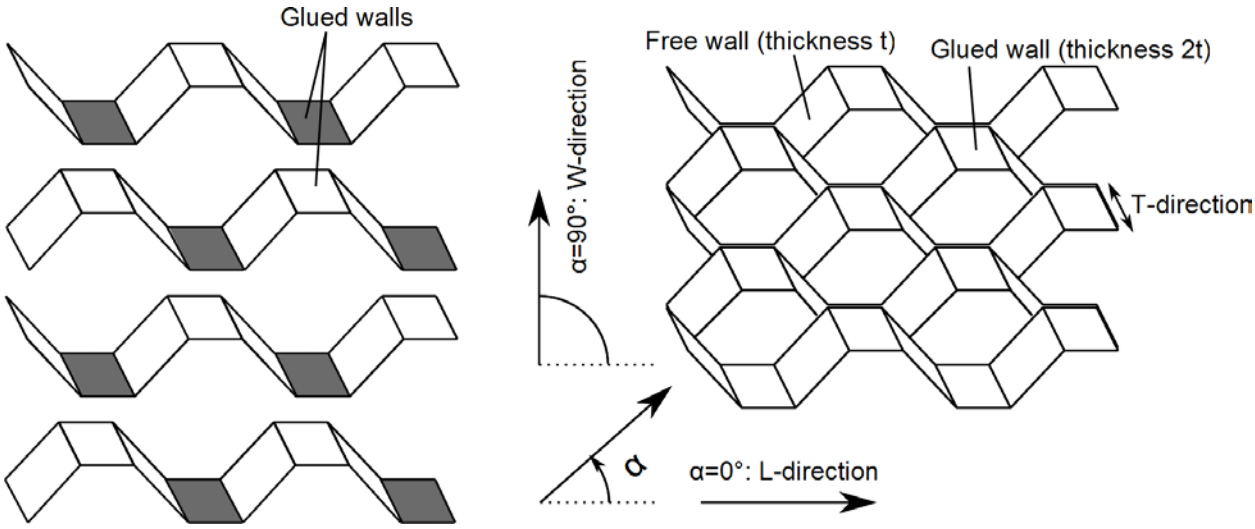

Fig. 2: Honeycomb core with notations

1.3 Stresses in Honeycomb Sandwich Structures

A sandwich panel, which is exposed to a transverse load, is subjected to different stress types: The face sheets are mainly subjected to tension and pressure loads, and the core to shear and pressure loads.The tensile stress in the face sheets can lead to cracks in the face sheets, which was examined in another project [9] and is not covered in this report (this failure mode has not occurred in the experiments of this work).

The core of sandwich panels fails usually due to shear or compression stress. The shear and compression stress distribution in a sandwich panel's core is illustrated in Fig. 3 for a typical three-point bending test. Depending on the cell geometry and the load application, the shear or the compression stresses are prevailing with the prevailing type of stress being responsible for the core failure. The distribution of the stresses in Fig. 3 was simulated with the ANSYS finite element software. The shear stress is maximal next to the point of the middle force application. The compression stress in the core reaches a maximum just below the middle load. Core indentation occurs when the compression stress surpasses the buckling strength of the honeycomb core. In this case, the structure fails locally due to the core's buckling (Fig. 3).

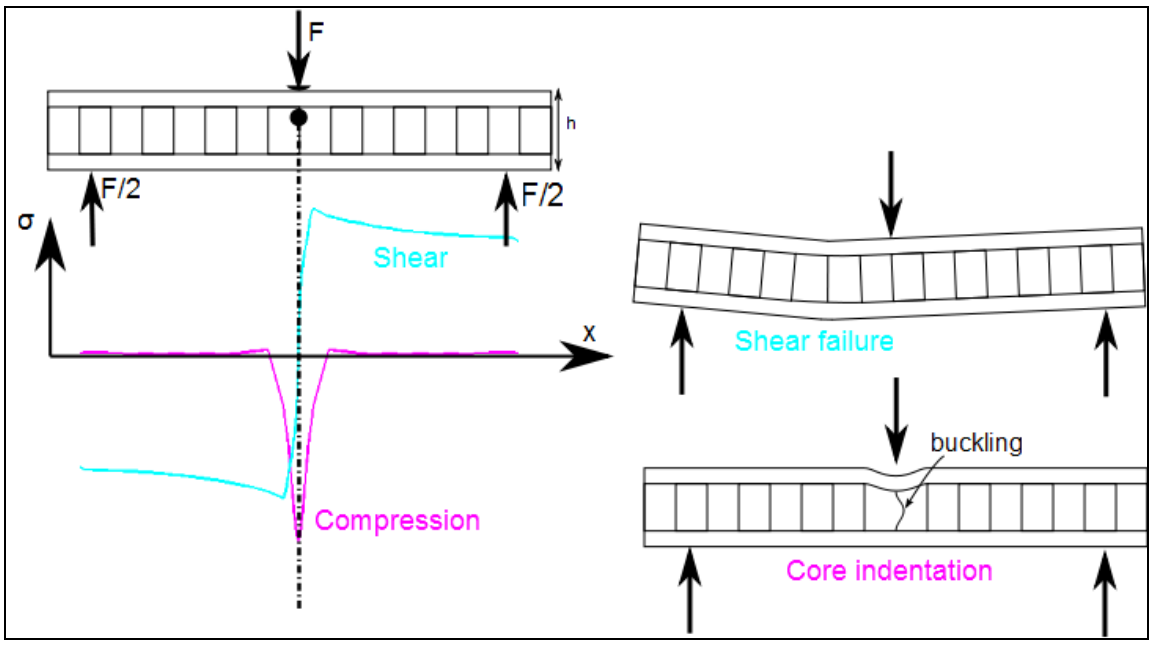

Fig. 3: Stress distribution and failure modes of the honeycomb core

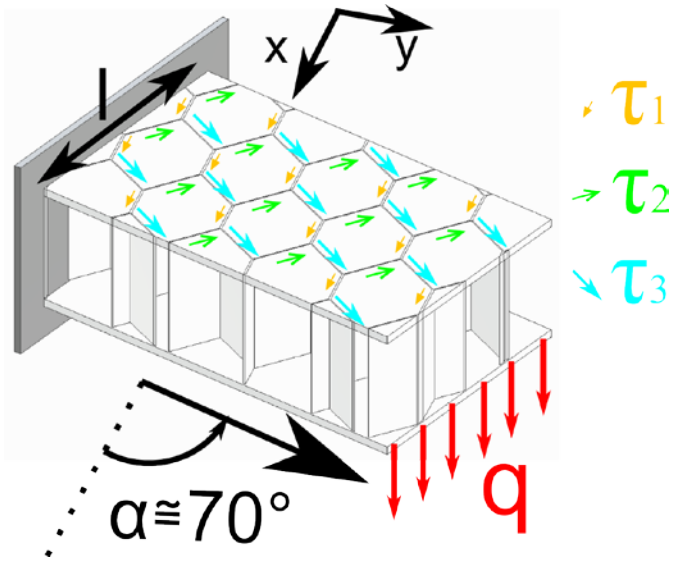

Fig. 4: Top view of a clamped sandwich structure loaded by a transverse force (Shear stresses τ_1, τ_2 and τ_3 are not identical)

A clamped sandwich structure with a core orientation of α=70° and loaded by a transverse force q is illustrated in Fig. 4. The honeycomb core is composed of three-angle cell walls, which are subjected to different in-plane shear stresses τ_1, τ_2 and τ_3 as shown in Fig. 4. Depending on the orientation of the orthotropic core, yet the shear stresses τ_1, τ_2 and τ_3 do not change synchronously. The average stresses of τ_1, τ_2 and τ_3 in dependency of the angle α are illustrated in Fig. 5 for a sandwich panel having a width of 76-mm, a cell size of 6.4-mm and a transverse force of 100N (Derivation can be found in [12]).

Fig. 5 shows that the highest stresses occur at 62° from the L-direction, which makes it the weakest direction (and not the W-direction as generally assumed). In L-direction (0°) the stresses τ_1, τ_2 and τ_3 have the same value and so the stresses are perfectly distributed in the structure. That is why the stresses in L-direction (the strongest direction) are about half of the maximal stresses in 62°-direction [12].

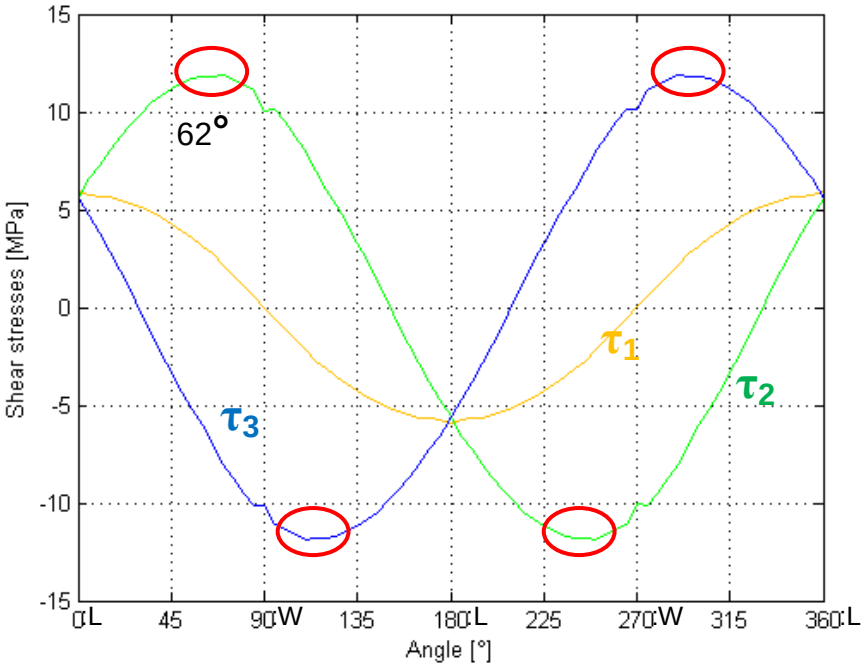

Fig. 5: Shear stresses τ_1, τ_2 and τ_3 in dependence of the orientation angle α

2 *Materials* and Dimensions of the Investigated Structures

2.1 Material Properties

The examined sandwich structure consists of three different materials:

- Glue ST Epoxy
- Aluminium alloy AlMg3 H44 (AW 5754) for the face sheets
- Aluminium alloy AlMn1Cu H19 (AW3003) for the honeycomb structure

The mechanical properties of the different materials are listed in Table 1.

	Young's modulus	Tensile yield strength	Tensile ultimate strength	Ultimate strain
AlMg3 H44*	70'500 MPa	200 MPa	270 MPa	5%
AlMn1Cu H19*	69'500 MPa	190 MPa	265 MPa	2,5%
Glue ST Epoxy**	1'900 MPa		50 MPa	

Table 1: Mechanical properties of the materials used in the sandwich panels
*: experimental Data
**: from Datasheet

Some cyclic tensile fatigue tests (Fig. 6) were conducted at a load ratio of R=0.1 (thickness of material doesn't allow compresion) with the core material AlMn1Cu H19 to get the S-N curves (Fig. 7). The very thin samples were produced by stamping (Shape according to ASTM D638). The S-N curve for shear stresses was derived from the tension curve, by moving the curve downwards by the factor $\sqrt{3}$ according to the Von Mises criterion (at 10^6 cycles). The slope k is changed by the factor 1.6 (from 8 to 13) according to the FKM-guideline [11] (this is an assumption, which is confirmed for this material in section 6).

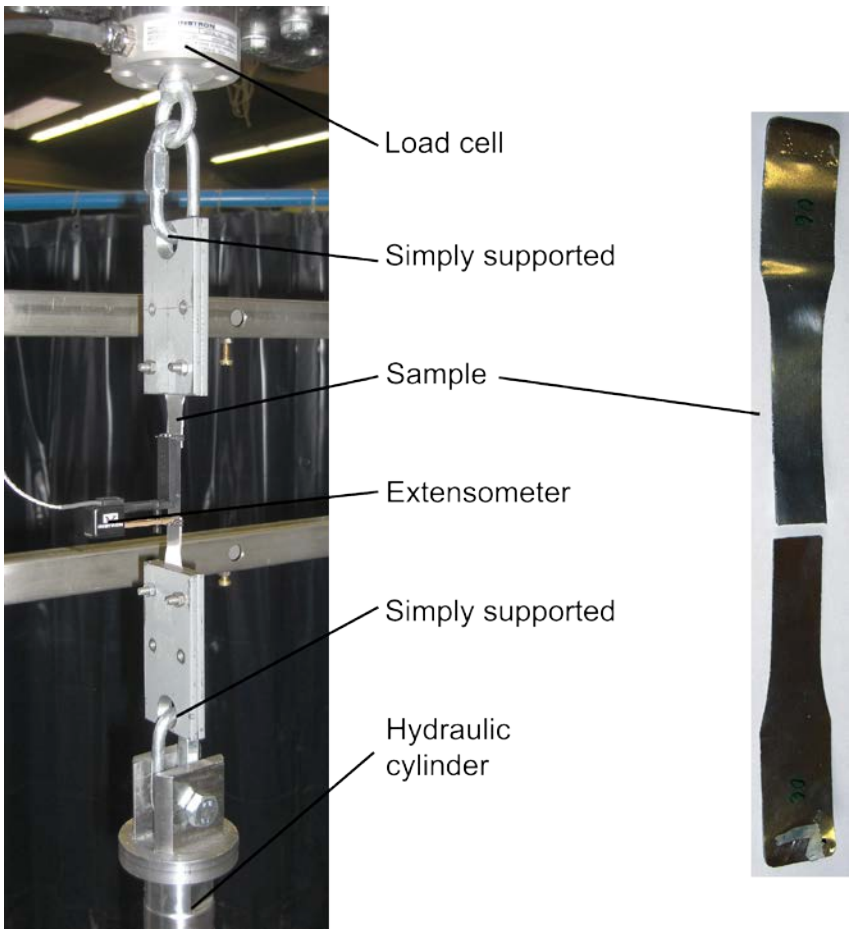

Fig. 6: Tensile fatigue test setup used for the cyclic material testing (left) and broken sample (right)

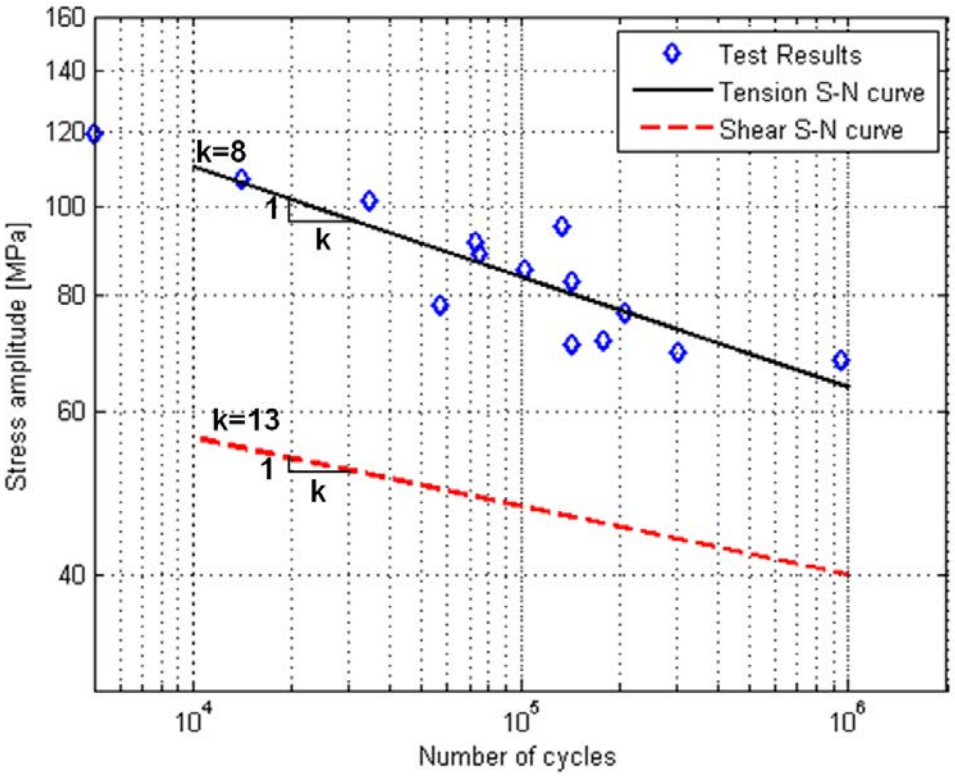

Fig. 7: S-N curves for a load ratio of R=0.1 and a failure probability of 50% (Tension curve interpolated, shear curve calculated)

2.2 Properties of the Core

The properties of the core structure differ strongly from the aluminium material properties used for the core's production. The physical properties of the core are shown in Table 2. The elasticity constants of the core can be derived from literature [1, 13].

Cell size	**6.4mm**	**9.6mm**
Honeycomb density	82kg/m^3	55kg/m^3
Material	Aluminium	Aluminium
Panel height h	10mm	10mm
Face sheet thickness	0.6mm	0.6mm
Honeycomb foil thickness t	0.08mm	0.08mm
$\mathbf{E_X}$	1.47 MPa	0.44 MPa
$\mathbf{E_Y}$	0.48 MPa	0.14 MPa
$\mathbf{E_Z}$	2124 MPa	1426 MPa
$\boldsymbol{\nu_{XY}}$	0.57	0.57
$\boldsymbol{\nu_{YZ}}$	0.000074	0.000033
$\boldsymbol{\nu_{XZ}}$	0.00023	0.00010
$\mathbf{G_{XY}}$	0.71 MPa	0.21 MPa
$\mathbf{G_{YZ}}$	252 MPa	169 MPa
$\mathbf{G_{XZ}}$	523 MPa	354 MPa

Table 2: Orthotropic properties for the core

3 Description of the different experimental set-ups

3.1 Three-Point Bending Tests

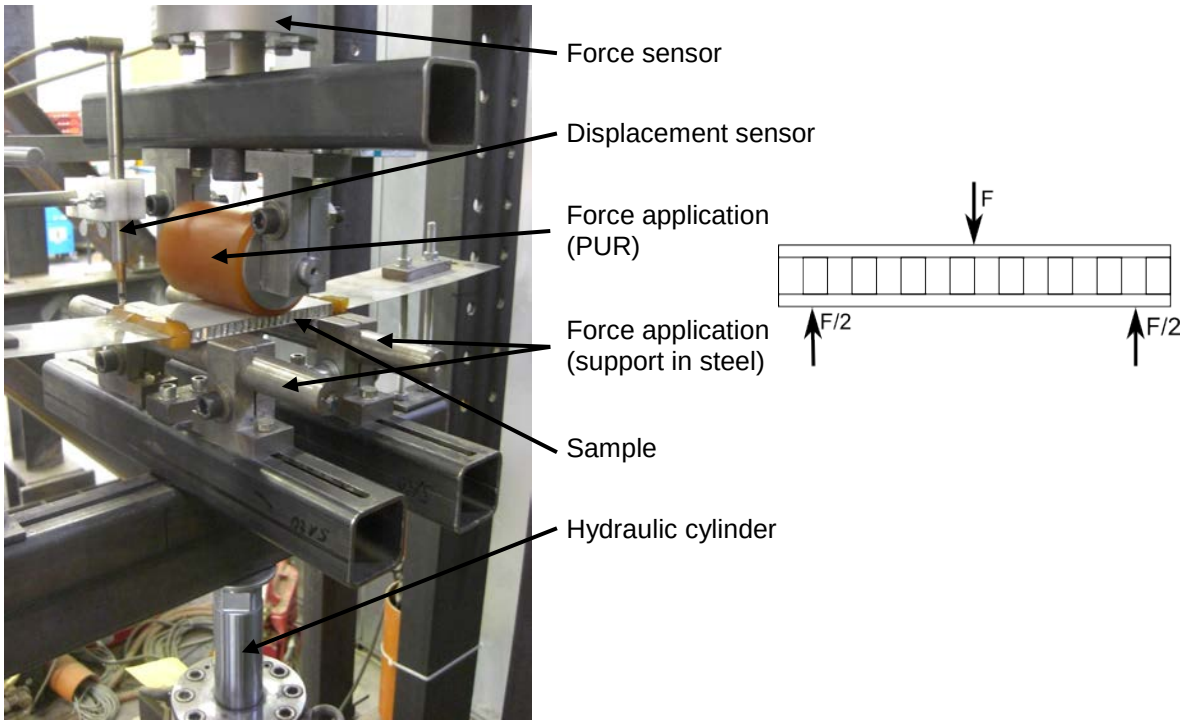

Fig. 8: Three-point bending setup used for fatigue testing

Dynamic 3-point bending tests were performed to provoke core failure. The test setup is powered by a hydraulic cylinder from Instron Structural Testing Systems (IST). Fig. 8 is showing the test setup

including the sensors. The displacement of the support in steel is measured by an inductive sensor, which is also detecting the damage. The samples were loaded in the three-point bending test with a sinusoidal load (regulated by the force sensor) with constant amplitude at a power ratio of R=0.1. The excitation was force-controlled. The specimens fail in the core due to the shear stresses, like shown in section 6.1.

3.2 Food-Cart Roller Test

Another common fatigue test for sandwich structures is the “Food-Cart Roller Test” [14, 15]. This test consists of a plate, which is charged with weight loads and rolls on three wheels on a sandwich structure (Fig. 9). The wheels move in a circle, thus they cross the fixed internal core structure in every orientation angle. There are two sandwich panels screw-fixed to the rig, like illustrated in Fig. 9. This test simulates a cart which is rolling on a floor panel, e.g. in a plane. The face sheets and the adhesive layer are not failing in this test as well, but the core structure is failing due to the shear stresses, like shown in section 6.2.

During this test, several values can be measured: The vertical displacements of the panel are measured with displacement sensors at several locations. Some strain gauges can be glued on the panel, in order to measure the strains in the sandwich structure’s plates. The vertical displacement of the rotating plates is measured by a contactless capacitive sensor. By means of this displacement value, it is possible to detect damage to the structure. Finally, the number of revolutions is also recorded.

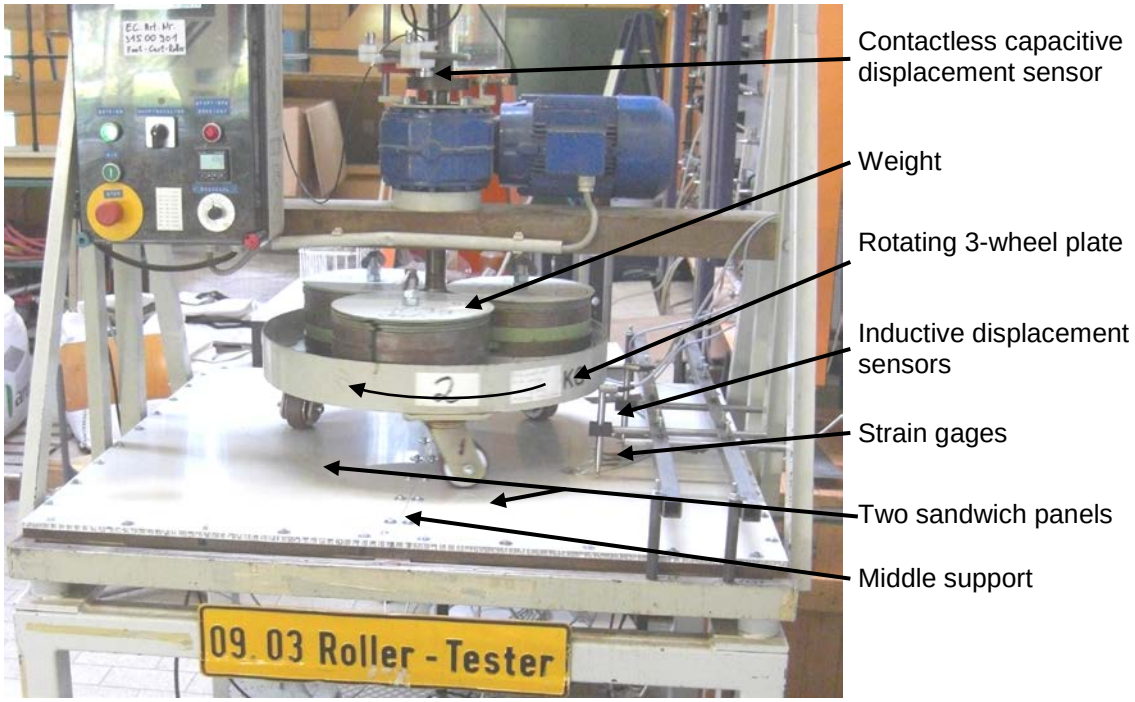

Fig. 9: Food-Cart Roller testing rig

The Food-Cart Roller tests were executed with the same sandwich panels as described in Table 2. The parameters of the testing rig are listed in Table 3.

Panel size	543mm x 1003mm
Testing speed	20 rev/minute
Wheel diameter	76mm
Wheel width	32mm
Wheel hardness	80 +- 5 Shore A
Diameter on which the wheels run	508 mm

Table 3: Dimensions of the Food-Cart Roller testing rig

4 Simulations

4.1 Three-Point Bending Simulation

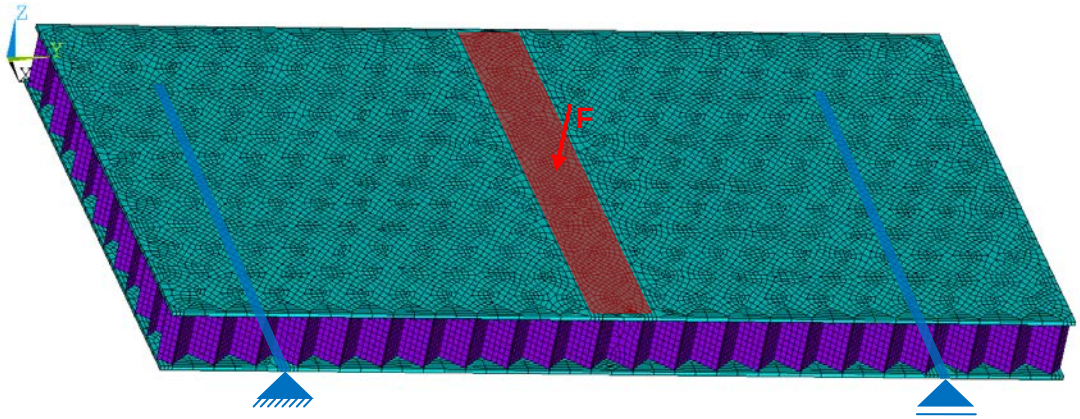

Fig. 10: Finite element model of the three-point bending test

A model of the sandwich structure was created with the ANSYS finite element software. The core structure was modeled with shell281 elements, having eight nodes with 6 degrees of freedom each. Shell281 elements are also suitable for large deformations and plastic behavior. The face sheets were modeled with solid95 elements, volume elements with 20 nodes with 3 degrees of freedom each. Linear finite element analyses are appropriate, because no big plastic effects are occurring during the investigations (minimum 10^4 cycles). No imperfections were included in the structure as the influence of the small imperfections had been proved to be negligible [16]. The distributed load was applied on the same area as in the experiments (pressure load initiated at a width of approx. 10mm, as shown in Fig. 10).

4.2 Food-Cart Roller Simulation

The dimensions of the panels of the Food-Cart Roller Test are much bigger than the panels of the three-point bending tests. In order to mesh the honeycomb core of the Food-Cart Roller Test, a huge number of elements is necessary, which would lead to exploding computation times.

The number of elements is reduced by replacing the honeycomb core with a homogeneous core with orthotropic properties (properties given in Section 2.2). The resulting displacements (not the stresses) of the homogeneous core simulation are approximately the same as the solution of the real honeycomb core. The homogeneous core was modeled with solid95 elements.

The equivalent stress of the homogeneous model showed that the stresses are only critical at the position of the load application. In order to get the stresses in the honeycomb core at this location, a submodel was created (Fig. 11). The boundary conditions for the submodel are extracted from the homogeneous model. The load application in the homogeneous model and the submodel are identical, hence the deformations are also identical. However, the stresses in the homogeneous core are very different from the true stresses in the structure. As a result it is only possible to examine the stresses in the submodel's honeycomb core where the cells are modeled by shell elements, i.e. all cells are modeled.

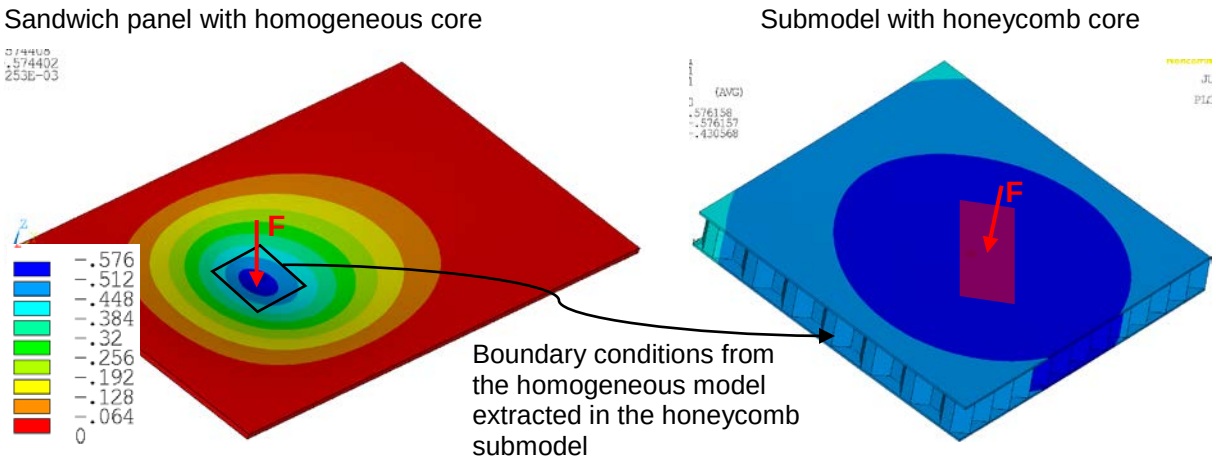

Fig. 11: Sandwich panel with homogeneous core and submodel with honeycomb core modeled with shell elements (vertical displacement displayed)

4.3 Load Application

An important part of the simulation is to model the load application in a convenient way on the specimen. The load application in the tests is realized by a roll made of polymer polyurethane, which has nonlinear properties. The pressure distribution under the load application is measured with a Fujifilm pressure film. The red color of the pressure film shows the pressure distribution on the contact region. The most important parameter of this measurement is the size of the area on which the load is applied. The investigations showed that the slightly unequal load distribution over the area has no considerable influence on the results. However, if an incorrect assessment of the load area is made, there is a big impact. Therefore, in the simulation, the load was applied perfectly distributed on an area with the same size as in this measurement.

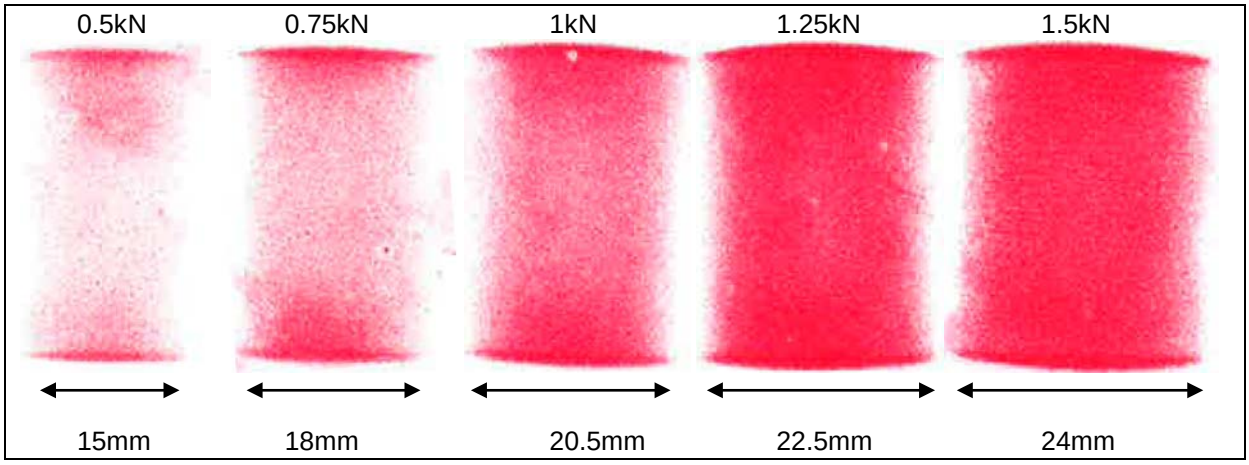

Fig. 12: Pressure distribution under the wheel depending on the load (Food-Cart Roller Test)

4.4 Core Indentation (Buckling of the Core)

In Section 1.3 it was shown that the honeycomb structure could fail in the mode of core indentation. Physically, core indentation of honeycomb panels means that the cell walls are buckling. The buckling process induces bending stresses in the cell walls, including high tensile stresses. These tensile stresses have a very negative influence on the core's fatigue behavior, i.e. the crack initiation phase immediately becomes very short. Therefore, it is reasonable not to tolerate the buckling of the core. In real applications, core indentation is usually avoided by reinforcing the panel at the position of the load application.

Good lifetime predictions can only be made if no buckling occurs in the honeycomb core. Therefore the buckling effect of the core has to be analyzed, which can be done in two different ways, using the finite element method: first, by a buckling analysis that calculates the theoretical buckling load for a perfect elastic system (Euler analysis), or, alternatively, by evaluating the buckling load in a nonlinear simulation. The simulations done during this project showed that both methods lead to similar results, due to the small deformations. Therefore a nonlinear simulation is not necessary.

5 Fatigue Analysis

The fatigue analysis of an aluminium honeycomb sandwich's core structure should be as follows:

- Determine the buckling load of the core in a buckling finite element analysis (considering geometric nonlinearities). To avoid buckling the load applied must not reach this value.
- Determine the stresses in a static finite element analysis with a homogenized core and a coarse mesh (Pure elastic simulation).
- Locate the critical points (e.g. in a contour plot of shear stresses as these stresses are predominating).
- At the critical point determine the exact stresses in a submodel with shell elements and a fine mesh (in this work, pure elastic simulations are enough, because no buckling is occurring and stresses are below yield point).
- Calculate the honeycomb core's lifetime, using the FKM-guideline [11].
- If possible, confirm the results by tests.

5.1 Buckling Loads

Before doing a fatigue analysis, it is important to make sure that there is no buckling in the core. Therefore, there were buckling analyses made for the tree-point bending test and the food-cart roller test. The buckling loads of the specimens with different core orientations and different cell sizes are shown in Table 4. It can be seen that the buckling loads are in this case higher than the failure loads calculated in the next section, hence no buckling will occur.

	Buckling load from FEM for the 6.4mm cell	**Buckling load from FEM for the 9.6mm cell**
3-point bending L-direction	3700N	2300N
3-point bending W-direction	3150N	1950N
3-point bending 62°-direction	3100N	1925N
Food-cart roller 62°-direction	1950N	1200N

Table 4: Buckling loads of the three-point bending test

5.2 Three-Point Bending Fatigue Analysis

After proving that there is no buckling of the core, a static finite element analysis can be made, followed by a fatigue prediction using the results of this analysis. At locations of the load application, the compression stress is predominating, and close to the load application, the shear stress predominates as shown in Fig. 3. When there is no buckling of the core, the most damaging stress component in the core is the shear stress. Therefore, the critical location can be determined from a shear stress contour plot. A fatigue prediction can be made for this location, using the FKM-guideline [11].

In Fig. 13 the different stress components in the honeycomb core are illustrated for the specimen with the core oriented in W-direction and a load amplitude of 787N (randomly chosen). The fatigue prediction was made according to the FKM-guideline for shell structures. Table 5 shows the calculation steps for this example, by using the FKM-guideline [11]. For 80'000 cycles, the degree of utilization is 1. As a result the failure of the structure is predicted after 80'000 cycles according to the FKM-guideline [11].

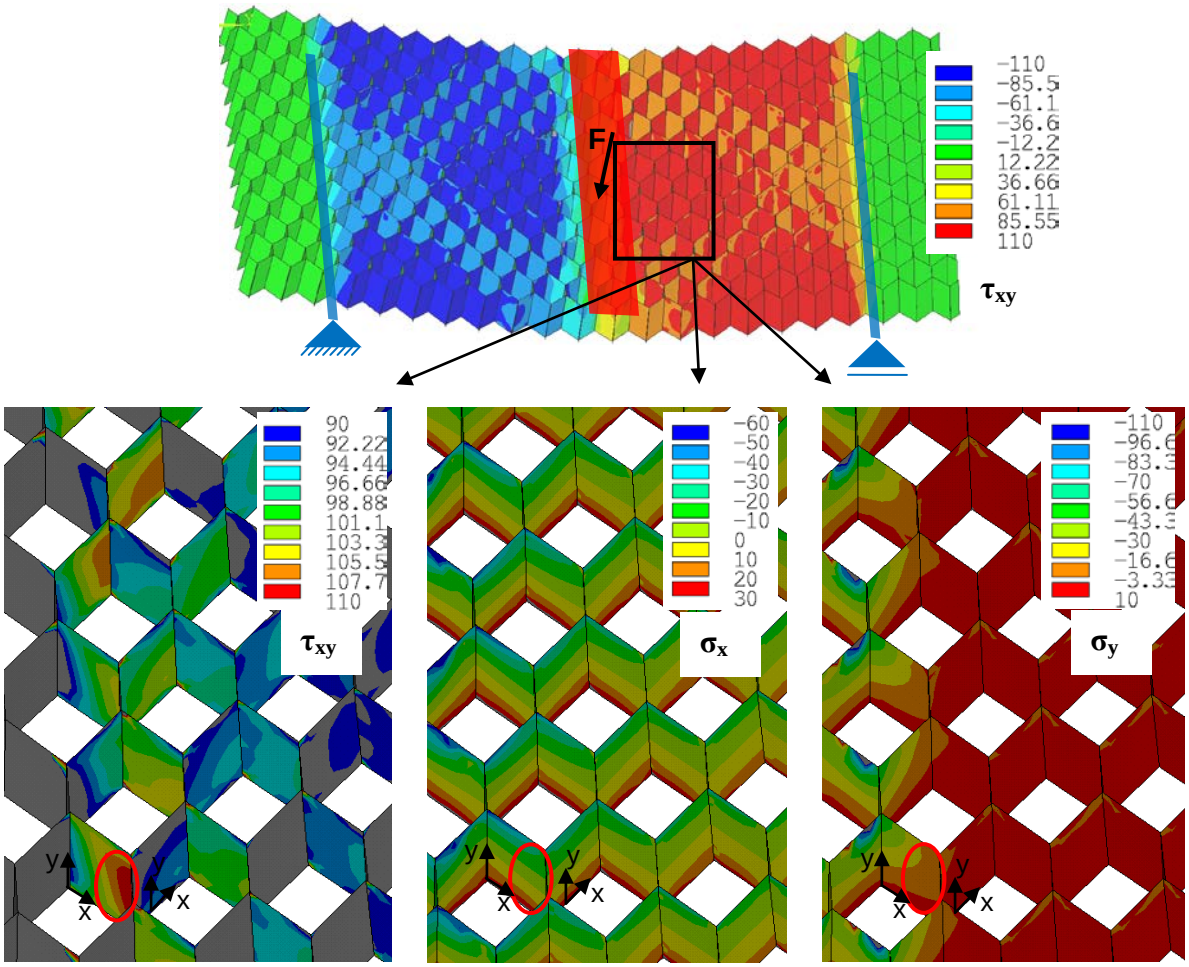

Fig. 13: Stresses in the core during the 3-point bending test (Load amplitude=787N, W-direction, element coordinate system)

Maximum shear stress at the critical location (Fig. 13)	$\tau_{Max} = 108MPa$
Shear stress amplitude at the critical location (R=0.1)	$\tau_a = (1-R)/2 \cdot \tau_{Max} = 48.6MPa$
Normal stress amplitudes at the critical location	$\sigma_x \approx 0$ and $\sigma_y \approx 0$
Material resistance at a load ratio of R=0.1 (at 10^6 cycles in Fig. 7)	$\sigma_{W,zd} = 63.9MPa$
Material resistance at a load ratio of R=0.1	$\tau_{W,s} = \sigma_{W,zd} / \sqrt{3} = 40MPa$
Construction factor (very good surface, no stress gradient perpendicular to the surface)	$K_{WK,\tau} = \frac{1}{n_\tau} \cdot (1 + \frac{1}{\tilde{K}_f} \cdot (\frac{1}{K_{R,\tau}} - 1)) \cdot \frac{1}{K_V \cdot K_S} = 1$
Component resistance at a load ratio of R=0.1	$\tau_{WK} = \tau_{W,s} / K_{WK,\tau} = 40MPa$
Mean stress factor (R=0.1 during material and component test)	$K_{AK,\tau} = 1$
Internal stress factor (assumption)	$K_{E,\tau} = 1$
Component endurance limit	$\tau_{AK} = K_{AK,\tau} \cdot K_{E,\tau} \cdot \tau_{WK} = 40MPa$
Service strength factor (k=13, N=80'000)	$K_{BK,\tau} = \left(\frac{N_D}{N}\right)^{1/k} = 1.21 \qquad (N_D = 10^6)$

Component fatigue strength	$\tau_{BK} = K_{BK,\tau} \cdot K_{E,\tau} \cdot \tau_{AK} = 48.69 MPa$
Safety factor (50% reliability)	$j = 1$
Cyclic degree of utilization	$a_{BK,\tau} = \frac{\tau_a}{\tau_{BK} / j} = 0.998$

Table 5: Fatigue prediction [11] at the location shown in Fig. 13: the component will fail after 80'000 cycles if the load amplitude=787N

In order to confirm the results, a different core orientation is analyzed. In Fig. 14 the different stress components for a specimen with a core orientation in L-direction and a load amplitude of 990N (randomly chosen) is illustrated. Similar to the W-direction, a fatigue prediction was made according to the FKM-guideline [11] for shell structures (Table 6). Although the load amplitude is higher in this example than in the example of the W-direction, the lifetime is higher as well (390'000 cycles v. 80'000 cycles).

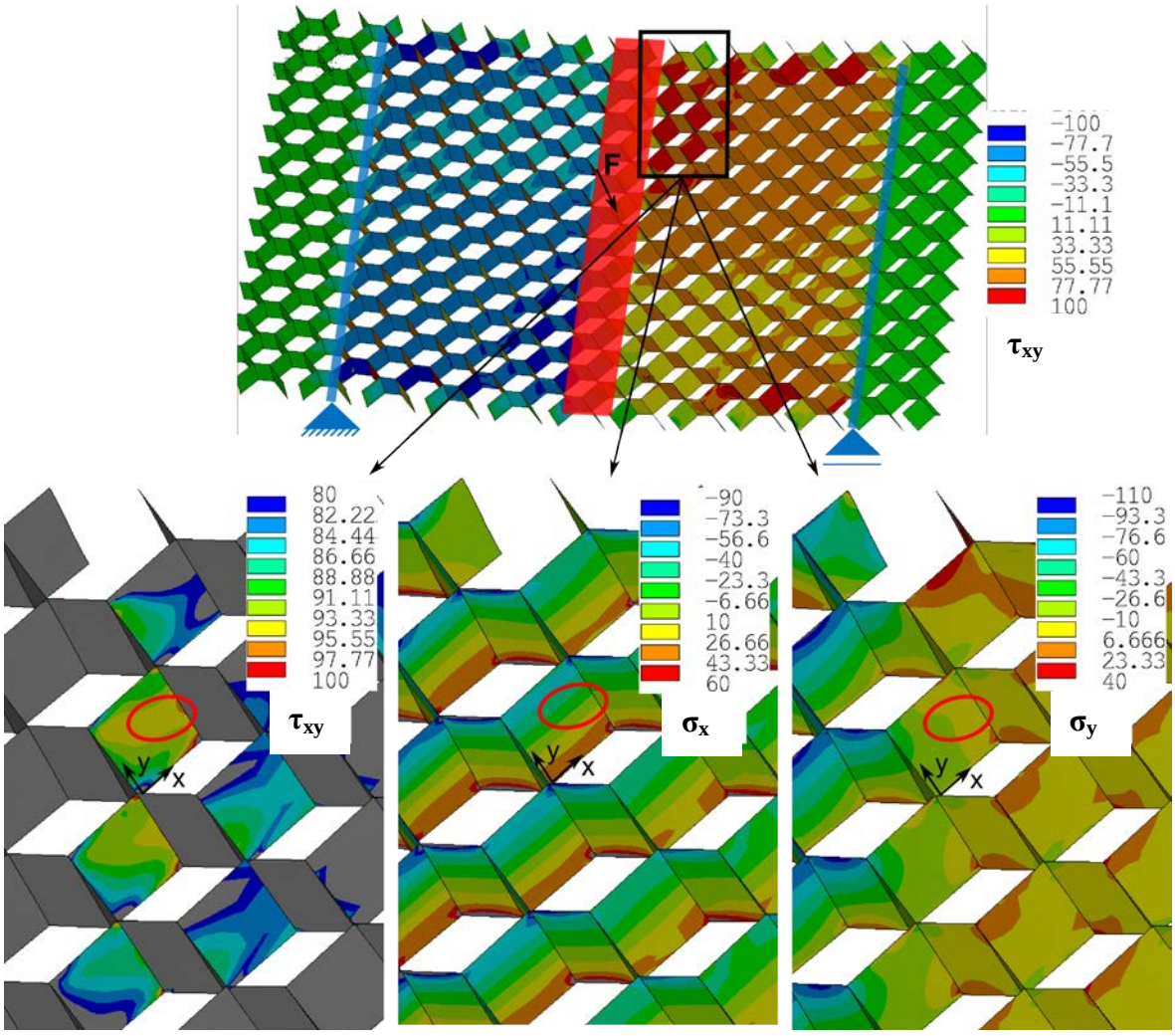

Fig. 14: Stresses in the core during the 3-point bending test (Load amplitude=990N, L-direction, element coordinate system)

Maximum shear stress at the critical location (Fig. 13)	$\tau_{Max} = 96MPa$
Shear stress amplitude at the critical location (R=0.1)	$\tau_a = (1-R)/2 \cdot \tau_{Max} = 43.2MPa$
Normal stress amplitudes at the critical location	$\sigma_x \approx 0 \text{ and } \sigma_y \approx 0$
Material resistance at a load ratio of R=0.1 (at 10^6 cycles in Fig. 7)	$\sigma_{W,zd} = 63.9MPa$
Material resistance at a load ratio of R=0.1	$\tau_{W,s} = \sigma_{W,zd} / \sqrt{3} = 40MPa$
Construction factor (very good surface, no stress gradient perpendicular to the surface)	$K_{WK,\tau} = \frac{1}{n_\tau} \cdot (1 + \frac{1}{\tilde{K}_f} \cdot (\frac{1}{K_{R,\tau}} - 1)) \cdot \frac{1}{K_V \cdot K_S} = 1$
Component resistance at a load ratio of R=0.1	$\tau_{WK} = \tau_{W,s} / K_{WK,\tau} = 40MPa$
Mean stress factor (R=0.1 during material and component test)	$K_{AK,\tau} = 1$
Internal stress factor (assumption)	$K_{E,\tau} = 1$
Component endurance limit	$\tau_{AK} = K_{AK,\tau} \cdot K_{E,\tau} \cdot \tau_{WK} = 40MPa$
Service strength factor (k=13, N=390‘000)	$K_{BK,\tau} = \left(\frac{N_D}{N} \right)^{1/k} = 1.07 \qquad (N_D = 10^6)$
Component fatigue strength	$\tau_{BK} = K_{BK,\tau} \cdot K_{E,\tau} \cdot \tau_{AK} = 43.2MPa$
Safety factor (50% reliability)	$j = 1$
Cyclic degree of utilization	$a_{BK,\tau} = \frac{\tau_a}{\tau_{BK} / j} = 1$

Table 6: Fatigue prediction [11] at the location shown in Fig. 14: the component will fail after 390’000 cycles if the load amplitude=990N

5.3 Food-Cart Roller Fatigue Analysis

During the rolling movement of the load application, the stress distribution in the honeycomb structure is very different to the three-point bending test. Therefore, the stress distribution in the sandwich panel’s core is investigated first. The stress distribution under the wheel in the rolling direction is illustrated in Fig. 15. The stresses were calculated by a finite element simulation. It is under the wheel that the compression stress is maximal and the shear stress is minimal. A buckling analysis shows that the compression stresses during this test are not leading to buckling of the cell walls (Table 4). Therefore, only a failure due to shear stresses was examined. The shear stresses have different signs in front and behind the wheel, so the shear stress ratio R on the wheel lane is -1. This is different concerning the left or the right side of the wheel (Fig. 16). On one side, the shear stress is always positive or zero, so the shear stress ratio R is zero at these locations. On the one side, the shear stress is always positive or zero, so the shear stress ratio R is zero at these locations. On the other side, the shear stresses are negative and the shear stress ratio R is -∞.

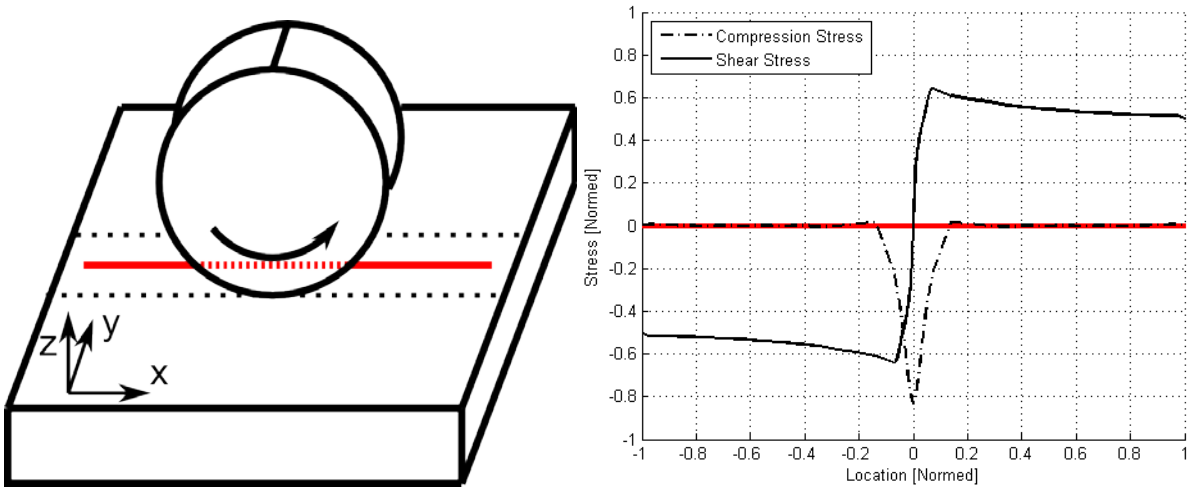

Fig. 15: Stress distribution, taken from a finite element analysis, in the core next to the wheels

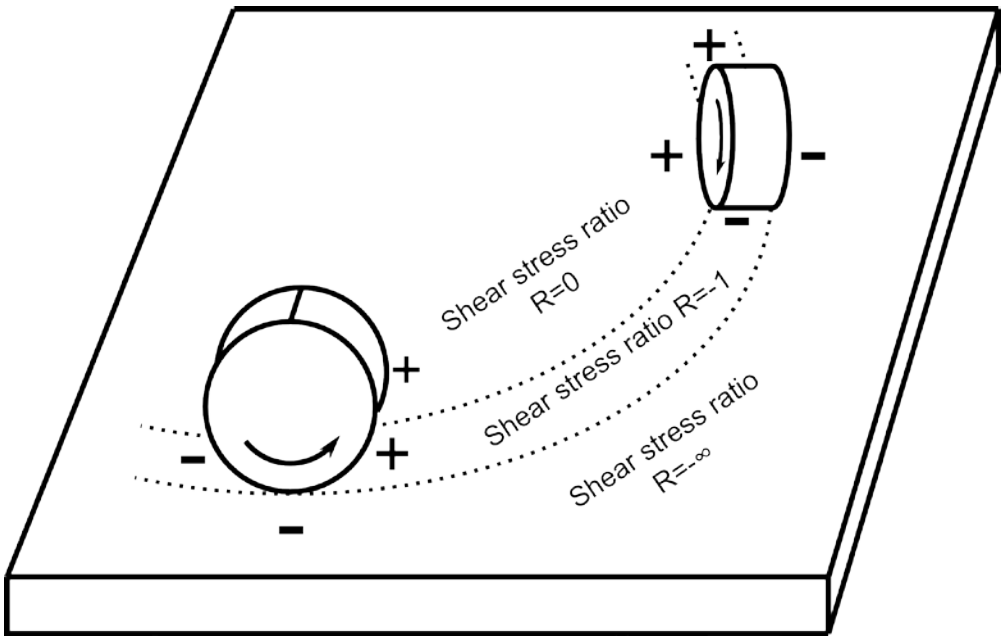

Fig. 16: Different stress ratios, depending of the location

Due to the different shear stress ratios in the structure, the shear stress amplitude has approximately double the size at the wheel lane than left or right of this lane. Hence the core will fail on the wheel lane, so the fatigue analysis must only be made at these positions.

In order to find the panel's weakest location during this test, some simulations were carried out. The size and the fixation of the panel had no big influence on the stresses in the core (on the stresses in the face sheets, however). The location of the load application has only a minor influence too. The core is failing at an angle of approximately 62° because the out-of-plane shear loads in 62°-direction produce the highest shear stresses as shown in Fig. 5 and Fig. 22.

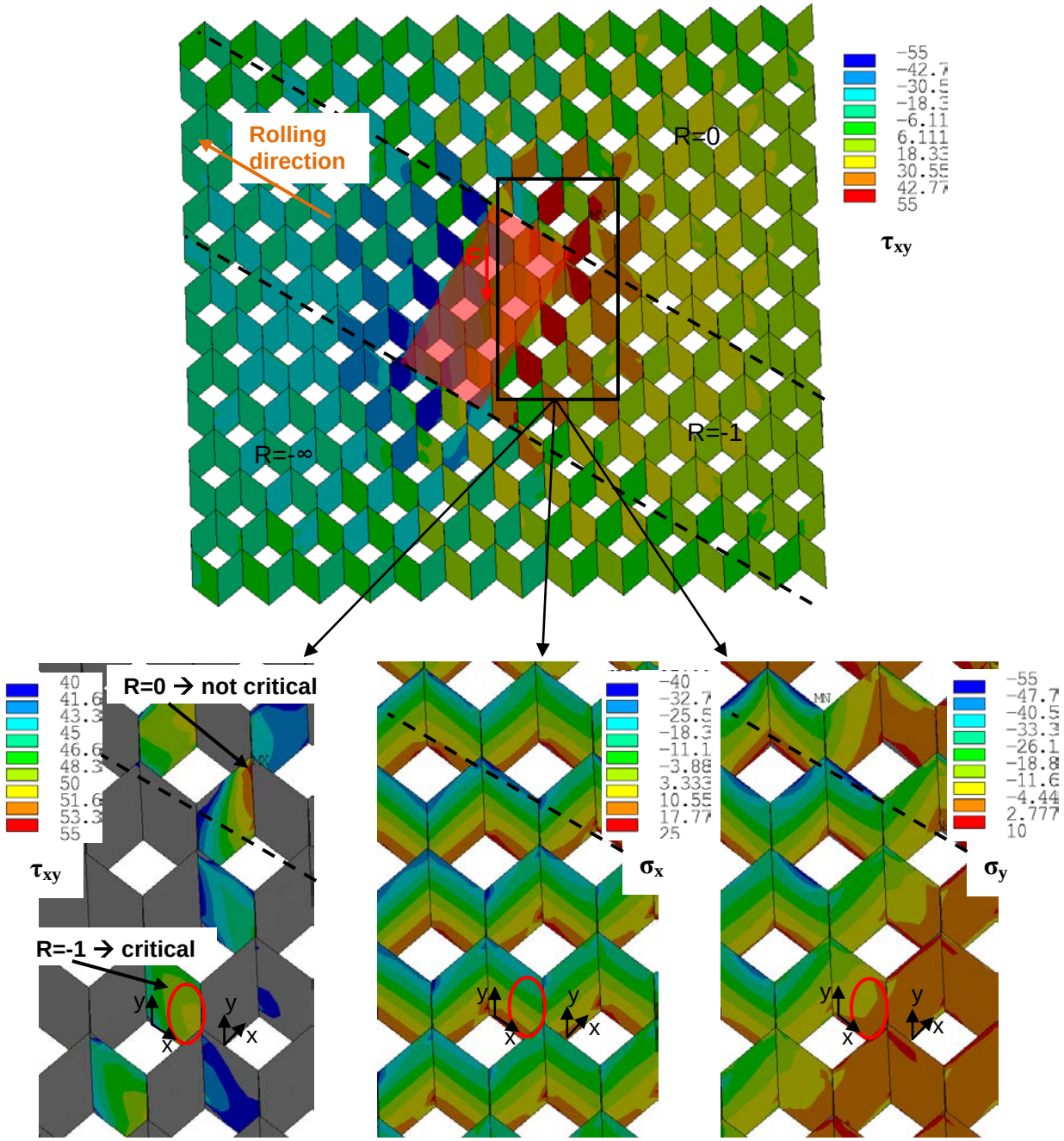

Fig. 17: Stresses in the core during the Food-Cart Roller Test (Load=560N per wheel at 62°, element coordinate system)

Fig. 17 shows the different stress components in the honeycomb core, at the moment when the wheel is at 62° (critical position) for the specimen loaded with a 560N (randomly chosen) per wheel. The critical walls are those where the shear stress ratio R is -1. The material tests have been conducted at a different stress ratio (R=0.1), whereupon a mean stress factor had to be defined [11]. The fatigue prediction was made according to the FKM-guideline for sheet-like components. Table 7 shows the calculation steps for this example. For 350'000 cycles, the degree of utilization is 1, so that the structure will fail after 350'000 cycles according to the FKM-guideline [11].

Shear stress amplitude at the critical location from Fig. 17 (R=-1)	$\tau_a = \tau_{Max} = 50MPa$
Normal stress amplitudes at the critical location	$\sigma_x = 0 \text{ and } \sigma_y = 0$
Material resistance at a load ratio of R=0.1 (at 10^6 cycles in Fig. 7)	$\sigma_{W,zd} = 63.9MPa$
Material resistance at a load ratio of R=0.1	$\tau_{W,s} = \sigma_{W,zd} / \sqrt{3} = 40MPa$
Construction factor (very good surface, no stress gradient perpendicular to the surface)	$K_{WK,\tau} = \frac{1}{n_\tau} \cdot (1 + \frac{1}{\tilde{K}_f} \cdot (\frac{1}{K_{R,\tau}} - 1)) \cdot \frac{1}{K_V \cdot K_S} = 1$
Component resistance at a load ratio of R=0.1	$\tau_{WK} = \tau_{W,s} / K_{WK,\tau} = 40MPa$
Mean stress factor (R=0.1 during material test and R=-1 during component test)	$K_{AK,\tau} = 1.14$
Internal stress factor (assumption)	$K_{E,\tau} = 1$
Component endurance limit	$\tau_{AK} = K_{AK,\tau} \cdot K_{E,\tau} \cdot \tau_{WK} = 45.9MPa$
Service strength factor (k=13, N=350‘000)	$K_{BK,\tau} = \left(\frac{N_D}{N} \right)^{1/k} = 1.1 \qquad (N_D = 10^6)$
Component fatigue strength	$\tau_{BK} = K_{BK,\tau} \cdot K_{E,\tau} \cdot \tau_{AK} = 50.3MPa$
Safety factor (50% reliability)	$j = 1$
Cyclic degree of utilization	$a_{BK,\tau} = \frac{\tau_a}{\tau_{BK} / j} = 0.995$

Table 7: Fatigue prediction [11] at the location shown in Fig. 17: the component will fail after 350’000 cycles if load amplitude=560N per wheel

6 Comparison Analysis / Test Results

6.1 Three-Point Bending Results

The fatigue tests lead to shear failure in the honeycomb core. No cracks could be detected in the adhesive layers (delamination) or in the face sheets (the experimental setup was chosen so that the tensile stresses in the face sheets are small). Cracks were initiated in the interior of the honeycomb core, which grew predominantly perpendicular to the first principal stress (Fig. 18). These cracks didn’t occur under the load, but some cells away from it, where the shear stress is maximal as shown in Fig. 3. This proves, that the failure is shear failure and not core indentation (core crush).

The amplitude of the cylinder displacement is nearly constant over the lifetime, mainly because the face sheets define the stiffness of a sandwich panel (the face sheets stay undamaged over the lifetime). Therefore, the displacement amplitude is not suitable to define a damage. A damage is defined in this work as an increase of the mean value of cylinder displacements by 50% of the displacement amplitude.

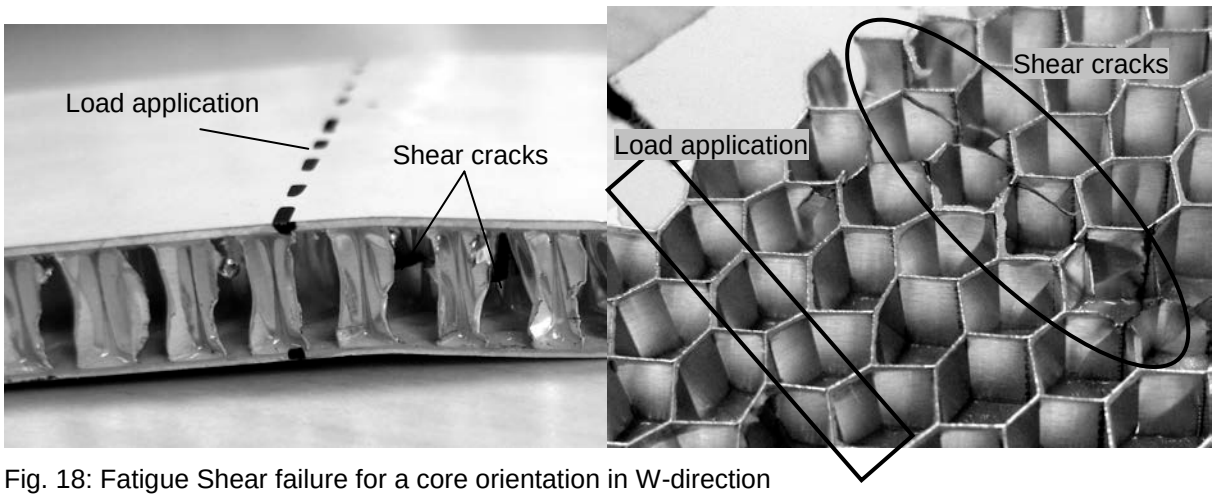

Fig. 18: Fatigue Shear failure for a core orientation in W-direction

In Section 1.3, we have seen that the angle of the core has considerable influence on the shear stresses in the structure. Therefore, the tests were made with three different angles: 0° (L), 62° and 90° (W). The 0° angle is the stiffest direction, 90° is the most compliant direction, and 62° is the weakest direction. (The stresses reach a maximum in the 62°-direction: Fig. 5.)

In Fig. 19, the fatigue prediction according to Section 5.2 is compared to the test results of these three angles for 6.4mm and 9.6mm cell sizes. The 62°-direction is the weakest one, as was explained in Section 1.3.

The ordinate of the fatigue diagram displays the force amplitude and not the stress amplitude at the location of the crack initiation. These two values are related, and the relationship is linear assuming Hooke's law and small deformations. The number of cycles on the abscissa corresponds to the number of cycles to complete failure of the part due to the fact that the cracks are invisible from outside.

Lifetime predictions for the cases examined in Fig. 19 are mostly conservative (error less than 14% in load amplitude). One explanation could be that the crack growth period is not considered in the fatigue prediction (the crack growth speed can vary, depending on the core orientation). Due to the scattering, which always occurs during fatigue tests, the results had been quite correctly predicted [17]. The slope of the predicted curves (k=13) are matching the results, which confirms the assumed slope.

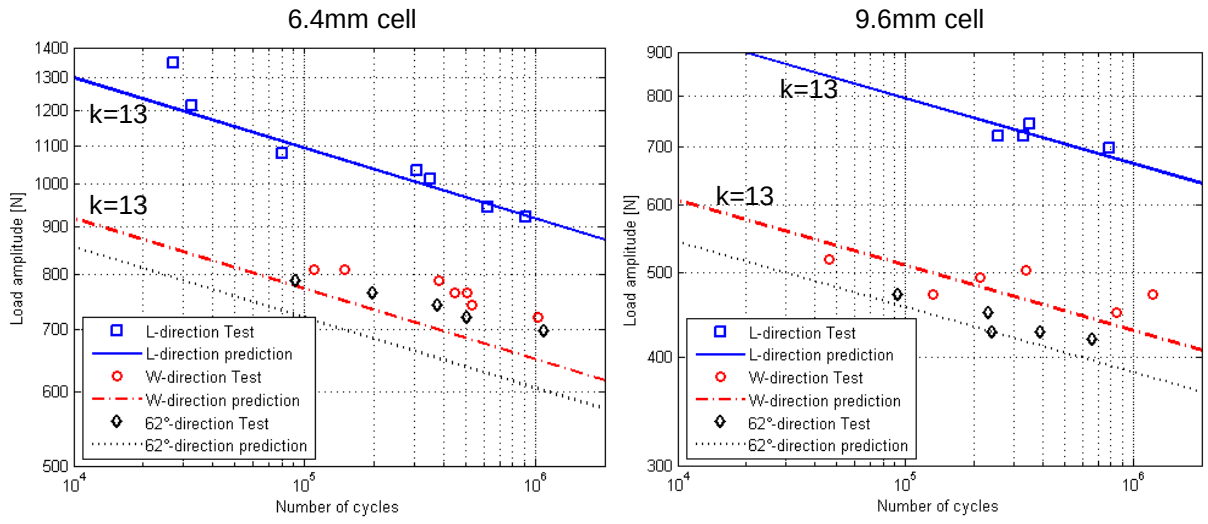

Fig. 19: Fatigue strength diagram for samples loaded in different directions and for 6.4mm and 9.6mm cell sizes

6.2 Food-Cart Roller Results

The testing configuration in Table 3 and the panel configurations in Table 2 always lead to the same damage mechanism. During the first 90% of the sandwich panel's total lifetime no damage could be detected. Afterwards some cracks occurred in the panel's core (Fig. 20). These cracks were located under the wheel lane and only in the walls, whose direction is almost parallel to the rolling direction. The simulations have shown that the shear stresses are prevailing (Fig. 17), which means this is a shear failure. In order to see the cracks, the plates had to be removed from the panel, meaning that the structure had to be destroyed. During the tests there was no sensor able to detect these minor cracks, which did not immediately lead to a total failure.

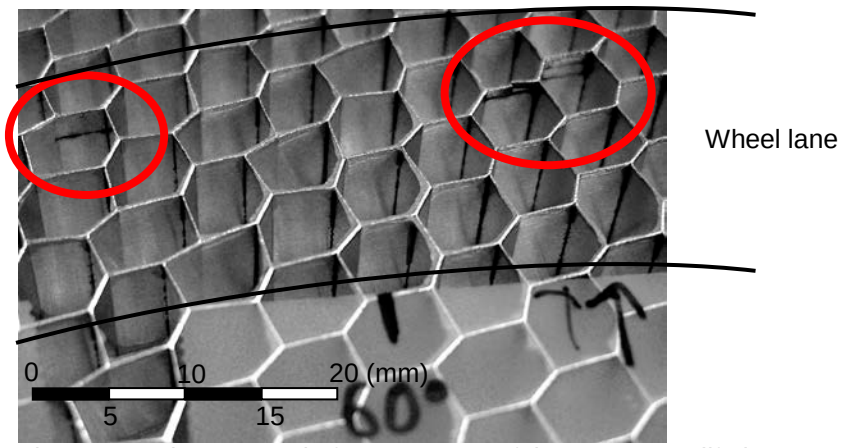

Fig. 20: Cracks occurred after over 90% of the structure's lifetime

When several cracks occur at the same location, the core cannot bear the load anymore and crushes (Fig. 21a). This crush is not the reason of the failure, but only the consequence of the previous shear failure. At this point, the damage is detectable from outside because a plastic deformation becomes measureable at the face sheet (but the panel can still carry loads).

After the crush of the core, the plate of the panel is subjected to considerably higher stresses, which finally lead to a total plate failure (Fig. 21b).

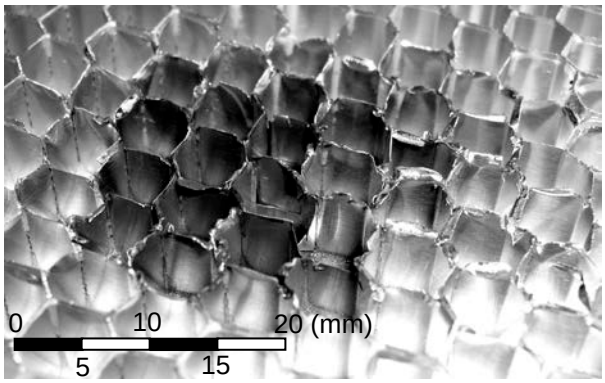

Fig. 21a: Location of core crush after cracking

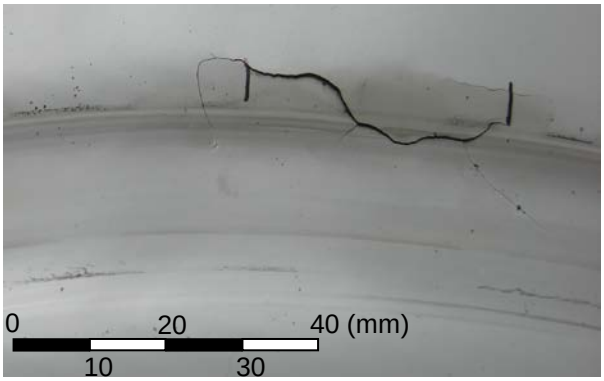

Fig. 21b: Crack in the coversheet of the pane after core crush.

The tests showed that the damage always occurs at about 62° from the support of the panel, meaning at 62° from the L-direction (Fig. 22). This corresponds perfectly well with the theoretical results shown in Fig. 5. The stresses reach their maximum, when the panel is loaded in this direction by a transverse shear load.

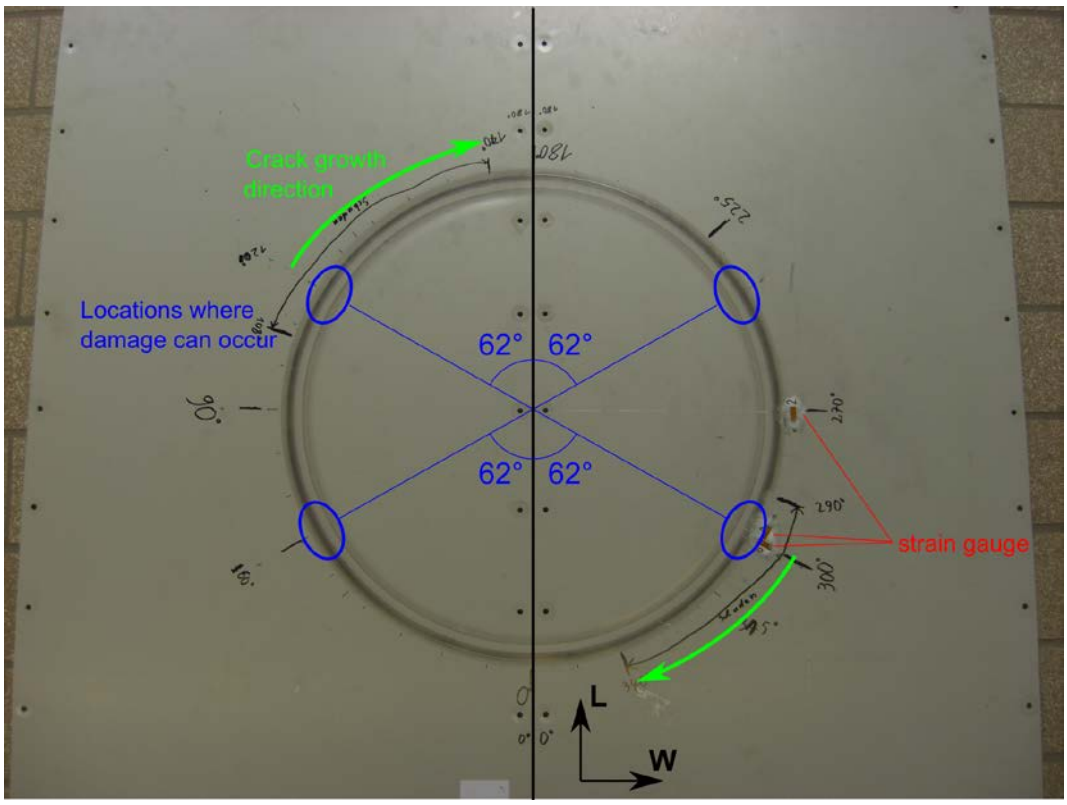

Fig. 22: Damage occurred at approximately 62° from the L-direction

The Food-Cart Roller Tests were executed at different load amplitudes. In Fig. 23, the fatigue prediction according to Section 5.3 was compared to the test results of 6.4mm and 9.6mm cell sizes. The abscissa illustrates the number of cycles before core failure occurred. As shown in Fig. 22, the panel has four potential damage locations. As a result it is theoretically possible that every test provides four measuring points in the fatigue strength diagram. In reality, however, to prevent damage being caused to the test equipment, the test often has to be stopped before the fourth location fails.

The crack growth period is not considered in the fatigue prediction in Fig. 23. Possibly due to this fact, the lifetime predictions for the examined cases were slightly conservative. The test for the 6.4mm cell size at around 700000 cycles shows an abnormal high lifetime. This difference is due to fluctuations in the material properties of the test setup. It could have been measured that the wheels of the load application were slightly softer in this test than in the other tests (wheels are replaced after each experiment).

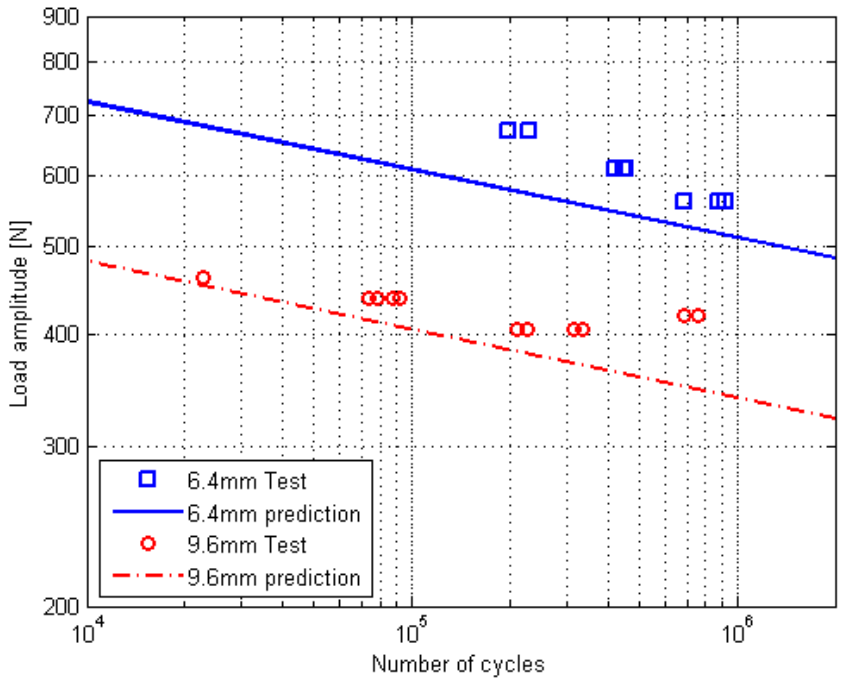

Fig. 23: Fatigue strength diagram of the Food-Cart Roller Test

7 Conclusions

There were two different failure modes of the aluminium honeycomb core structure examined: core indentation and shear failure. Core indentation induces the buckling of several honeycomb cells. In practice, components should be designed that no buckling will occur. The buckling load can easily be calculated with a finite element simulation. The shear failure mode can be analyzed by carrying out a static finite element analysis. Afterwards a lifetime analysis can be made using the FKM-guideline.

The lifetime predictions were confirmed by two different types of tests, namely the three-point bending test and the food-cart roller test. The differences between the predicted and tested lifetimes were inferior to 14% in load amplitude, with the predictions usually being conservative. The sandwich panels with a honeycomb core were investigated at different angles, and it was shown in theory and during testing that the 62° direction is the weakest.

8 Acknowledgement

The project was financially supported by Eurocomposites, Echternach, Luxembourg.

9 References

[1] Gibson, L.J.; Ashby, M.F.: “Cellular solids, Structure and properties”, Second edition, Cambridge University Press, 1997

[2] Staal, R.A.; Mallinson, G.D.; Jayaraman, K.; Horrigan, D.P.W.: “Predicting Failure Loads of Undamaged Sandwich Honeycomb Panels Subject to Bending”, Journal of Sandwich Structures and Materials, Volume 11, Issue 2-3, 2009, pp 73-104

[3] Zhang, J.; Ashby, M.F.: “The Out-of-plane Properties of Honeycombs”, International Journal of Mechanical Sciences, Pergamon Press, Volume 34, Issue 6, 1992, pp 475-489

[4] Sharma, N.; Gibson, R.F.; Ayorinde, E.O.: "Fatigue of Foam and Honeycomb Core Composite Sandwich Structures: A Tutorial", Journal of Sandwich Structures and Materials, Volume 8, Issue 4, 2006, pp 263-319

[5] Burman, M.; Zenkert, D.: “Fatigue of Undamaged and Damaged Honeycomb Sandwich Beams”, Journal of Sandwich Structures and Materials, Volume 2, Issue 1, 2000, pp 50-74

[6] S. Belouettar, S.; Abbadi, A.; Azari, Z.; Belouettar, R.; Freres, P.: “Experimental investigation of static and fatigue behaviour of composites honeycomb materials using four point bending tests”, Composite Structures, Volume 87, Issue 3, 2009, pp 265-273

[7] Belingardi, G.; Martella, P.; Peroni, I.: “Fatigue analysis of honeycomb-composite sandwich beams”, Composites Part A: Applied Science and Manufacturing, Volume 38, Issue 4, 2007, pp 1183-1191

[8] Berkowitz, C.K.; Johnson, W.S.: “Fracture and Fatigue Tests and Analysis of Composite Sandwich Structure”, Journal of Composite Materials, Volume 39, Issue 16, 2005, pp 1417-1431

[9] Bauer, J.: "Ermittlung von Schwingfestigkeitseigenschaften für Leichtbaupaneele mit Wabenstruktur", University of Luxembourg, Faculty of Science, Technology and Communication, PhD-FSTC-5-2008, 2008

[10] Bianchi, G.; Aglietti, G.S.; Richardson, G.: “Static and Fatigue Behaviour of Hexagonal Honeycomb Cores under In-plane Shear Loads”, Applied Composite Materials, Springer, 2011

[11] Hänel, B.; Haibach, E.; Seeger, T.: "Rechnerischer Festigkeitsnachweis für Maschinenbauteile aus Stahl, Eisenguss- und Aluminiumwerkstoffen – FKM-Richtlinie", 5th edition, VDMA Verlag GmbH, 2003

[12] Wahl, L.; Maas, S.; Waldmann, D.; Zürbes, A.; Frères P.:“ Shear stresses in honeycomb sandwich plates: Analytical solution, finite element method and experimental verification“, Journal of Sandwich Structures and Materials, Volume 14, Issue 4, 2012, pp 449-468

[13] Grediac, M.: “A finite element study of the transverse shear in honeycomb cores”, International journal of solids and structures, Volume 30, Issue 13, 1997, pp 1777-1788

[14] Boeing Specification BMS 4-17: Types I, II, III, IV. Boeing Material Specification, BMS 4-17U, 16 October 2007, pp 1-28.

[15] Douglas specification DAC 7954400. Douglas Specification, Size A, Code 88277, DAC 7954400, November 1985, pp 1-34.

[16] Wahl, L.; Zürbes, A.; Maas, S.; Waldmann, D.; Frères, P.; Wintgens, W.: Fatigue in Aluminium Honeycomb-core Plates; NAFEMS Benchmark Magazine, January 2011, pp 26-32

[17] Schijve, J.: "Fatigue of Structures and Materials", first edition, Kluver Academic Publishers, 2001